A Dynamically Adaptive Multilevel Wavelet Collocation Method for Solving Partial Differential Equations in a Finite Domain

OLEG V. VASILYEV AND SAMUEL PAOLUCCI

Department of Aerospace and Mechanical Engineering, University of Notre Dame, Notre Dame, Indiana 46556

A dynamically adaptive multilevel wavelet collocation method is developed for the solution of partial differential equations. The multilevel structure of the algorithm provides a simple way to adapt computational refinements to local demands of the solution. High resolution computations are performed only in regions where sharp transitions occur. The scheme handles general boundary conditions. The method is applied to the solution of the one-dimensional Burgers equation with small viscosity, a moving shock problem, and a nonlinear thermoacoustic wave problem. The results indicate that the method is very accurate and efficient. © 1996 Academic Press, Inc.

1. INTRODUCTION

A multilevel wavelet collocation method for the solution of partial differential equations has been developed recently by Vasilyev *et al.* [1]. The method utilizes the classical idea of collocation with the wavelet approximation. The authors suggest two different approaches of treating general boundary conditions: differential and integral. The differential approach uses standard wavelets as a basis and results in a differential–algebraic system of equations, where the algebraic part arises from the boundary conditions. The integral approach utilizes extended wavelets, which satisfy boundary conditions exactly. This approach results in a system of coupled ordinary differential equations. The method is tested on the one-dimensional Burgers equation with small viscosity and the solutions were compared with those resulting from the use of other methods. Their results indicate that the method is competitive with well-established numerical algorithms.

The multilevel wavelet collocation method proposed in [1] is based on the localization property of wavelets. Due to the fact that the zero-mean restriction plays no role in the algorithm, the method is applicable with any suitable basis function which has compact or essentially compact support in both physical and wavenumber spaces. Another very important aspect of the algorithm is its spectral accuracy [1]. Unfortunately while spectral convergence of the method is indicated by the numerical results, an analytical proof is lacking at this time.

Liandrat and Tchiamichian [2], Bacry *et al.* [3], Maday and Ravel [4], and Bertoluzza *et al.* [5] have shown that the multiresolution structure of wavelet bases is a simple and effective framework for spatially adaptive algorithms. In their Galerkin algorithms, they retain wavelets, whose coefficients are larger than a given threshold. In order to be able to track singularities they also retain wavelets that are adjacent to such regions. This adaptive procedure, based on the analysis of wavelet coefficients, allows them to follow the local structures of the solution.

In wavelet Galerkin algorithms nonlinearities can be handled using either the connection coefficients (see [3]) introduced by Beylkin [6, 7] or quadrature formulae (see [4]). The first approach is computationally expensive, due to the summations over multiple indices. The second one loses its accuracy due the approximate calculations of the scalar products (see [8]). In contrast, the treatment of nonlinear terms in the multilevel wavelet collocation method (see [1]) is a straightforward task due to the collocation nature of the algorithm.

Most of the wavelet algorithms for solving partial differential equations can handle periodic boundary conditions easily. The effective treatment of general boundary conditions is still an open question even though different possibilities of dealing with this problem have been studied. One approach is to use wavelets specified on an interval as suggested by Meyer [9] and Andersson *et al.* [10]. These wavelets are constructed satisfying certain boundary conditions. The disadvantages of this approach are inconvenience of implementation and wavelet dependence on boundary conditions. A more satisfactory approach is to make a change of variable in conjunction with the tau method to treat Dirichlet boundary conditions [4]. This approach may lead to some instabilities associated with the introduction of extra equations to treat boundary conditions, which in turn makes the system of equation overdetermined.

The main objective of the present work is to extend the collocation method developed in [1] and to incorporate the dynamically adaptive multilevel algorithm suggested by Liandrat and Tchamitchian [2]. The essential feature

of the multilevel wavelet collocation method is that the unknown functions themselves are solved for at collocation points, in comparison with the wavelet Galerkin algorithms which solve for wavelet coefficients. Even though wavelet coefficients do not explicitly enter into the final form of the wavelet collocation method, an adaptive algorithm analogous to the one proposed in [2] can be utilized.

The rest of the paper is organized as follows. In Section 2 we briefly review the wavelet interpolation technique developed in [1] with modifications which allow the extension to an adaptive algorithm. The dynamically adaptive method for solving partial differential equations is described in Section 3. Finally, in Section 4, the method is applied to the solution of the Burgers equation with small viscosity, the modified Burgers equation producing a moving shock solution, and a nonlinear thermoacoustic wave problem.

2. WAVELET INTERPOLATION

2.1. *Interpolation on a Regular Grid*

Let us consider a function $u(x)$ defined on a closed interval $\Omega \equiv [x_l, x_r]$. If we take $\psi_k^j(x) = a_j^{-1/2}\psi((x - b_k^j)/a_j)$, where $\psi(x)$ is a wavelet and $a_j = 2^{-j}a_0$, $b_k^j = (x_r + x_l)/2 + a_jb_0k$, $a_0 = 2^{-L}(x_r - x_l)/b_0$, and $L \in Z$, then it can be shown (see [1]) that there exist b_0, L, N_l, N_r such that $u(x)$ can be approximated as

$$u^J(x) = \sum_{j=0}^{J} \sum_{k \in Z^j} c_k^j \psi_k^j(x), \tag{1}$$

where $\{Z^j : -2^{L+j-1} - N_l, ..., 2^{L+j-1} + N_r\}$ and N_l, N_r are the number of external wavelets on each side of the domain Ω. Note that levels $j = 0$ and $j = J$ correspond respectively to the coarsest and finest scales present in the approximation, and the largest scale present in the approximation is determined by L.

For clarity of discussion we will call wavelets corresponding to the same j as wavelets at the j level of resolution, and for notational convenience we use the superscript to denote the level of resolution and the subscript to denote the location in physical space (with the exception of a_j).

We follow [1] in defining a set of collocation points $\{x_i^j : i \in Z^j\}$ in such a way that for any j $(0 \leq j \leq J - 1)$ the following relation between the collocation points at different levels of resolution is satisfied

$$\{x_i^j\} \subset \{x_i^{j+1}\}. \tag{2}$$

Then the operator $\mathbb{C}_{k,m}^{j,s}$ which maps the set of functional values at the J level of resolution into the set of wavelet coefficients at the j level can be constructed (see [1]):

$$c_k^j = \sum_{m \in Z^J} \mathbb{C}_{k,m}^{j,J}u_m^J, \quad 0 \leq j \leq J, k \in Z^j, \tag{3}$$

where

$$\mathbb{C}_{k,m}^{j,J} = \sum_{p \in Z^j} (A^{j,j})_{k,p}^{-1}\Delta_{p,m}^{j,J}, \quad 0 \leq j \leq J, k \in Z^j, m \in Z^J, \tag{4}$$

$$A_{i,k}^{l,j} = \psi_k^j(x_i^l), \qquad 0 \leq l, j \leq J, i \in Z^l, k \in Z^j, \tag{5}$$

$$\Delta_{i,m}^{j,J} = \begin{cases} R_{i,m}^{j,J} - \sum_{l=0}^{j-1}\sum_{p \in Z^j}\sum_{k \in Z^l} R_{i,p}^{j,J}A_{p,k}^{J,l}\mathbb{C}_{k,m}^{l,J}, \\ \qquad\qquad\qquad 1 \leq j \leq J, i \in Z^j, m \in Z^J, \\ R_{i,m}^{0,J}, \qquad\qquad j = 0, i \in Z^0, m \in Z^J. \end{cases} \tag{6}$$

In the above expressions the operator $(A^{j,j})_{k,p}^{-1}$ denotes the (k, p)-element of the inverse of the matrix $\mathbf{A}^{j,j}$ and the operator $R_{i,m}^{l,j}$ is the *restriction* operator defined as

$$R_{i,m}^{l,j} = \begin{cases} 1 & \text{for } x_i^l = x_m^j, \\ 0 & \text{otherwise.} \end{cases} \tag{7}$$

Since the restriction operator is known, than we have an explicit form for $\Delta_{i,m}^{0,J}$ and, consequently, for $\mathbb{C}_{k,m}^{0,J}$. Then using (4) and (6) the operators $\Delta_{i,m}^{j,J}$ and $\mathbb{C}_{k,m}^{j,J}$ are obtained recursively.

Next, the interpolation operator is defined as

$$u^J(x) = \sum_{i \in Z^J} I_i(x)u_i^J, \tag{8}$$

where

$$I_i(x) = \sum_{j=0}^{J}\sum_{k \in Z^j} \psi_k^j(x)\mathbb{C}_{k,i}^{j,J}, \quad i \in Z^J. \tag{9}$$

Since the collocation points are known, the interpolation operator can be constructed. In addition, using (1), (4), (5), (6), and (9) the mth derivative of the approximate function can be written as
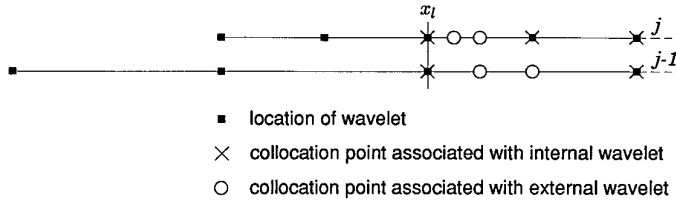
$$u^{J(m)}(x) = \sum_{i \in Z^J} D_i^{(m)}(x)u_i^J, \tag{10}$$

where

$$D_i^{(m)}(x) = \sum_{j=0}^{J}\sum_{k \in Z^j} \psi_k^{j(m)}(x)\mathbb{C}_{k,i}^{j,J}, \quad i \in Z^J. \tag{11}$$

Note that $D_i^{(0)}(x) = I_i(x)$.

All wavelets whose centers are located within the do-

FIG. 1. Locations of collocation points and wavelets near x_l for $N_l = 2$.

main, will be called internal wavelets; the other wavelets will be called external wavelets. Since every wavelet is characterized by its location b_k^j, then for internal wavelets these locations seem to be the most natural choice for collocation points, provided that wavelets are symmetric and nonzero at b_k^j. Nonsymmetrical wavelets can also be utilized, but in this case the choice for collocation points is not clear. Collocation points for external wavelets are located as described in [1]. Briefly, at any level of resolution j the collocation points corresponding to the external wavelets are located in the intervals $[x_l, x_l + b_0 a_j]$ and $[x_r - b_0 a_j, x_r]$ and are taken to correspond to the collocation points of possible internal wavelets of smaller scales. The placement strategy is illustrated in Fig. 1 with two external wavelets ($N_l = 2$).

We enumerate the collocation points in such a way that for any j $(0 \le j \le J)$ and $i, k \in Z^J$, $x_i^j < x_k^j$ if and only if $i < k$. Subsequently, it is easy to show that

$$x_{-2^{L+j-1}-N_l}^j = x_l, \quad x_{2^{L+j-1}+N_r}^j = x_r. \tag{12}$$

Up to this point we have indicated that $\psi(x)$ is a wavelet; however, we emphasize that the present method is applicable for any suitable function, provided it has compact or essentially compact support. In order not to cloud the discussion we will keep referring to our functions as wavelets, keeping in mind that true wavelets have additional properties. In fact, we illustrate the method using the correlation function of the Daubechies scaling function of order 5 with $b_0 = 1.0$ (see Beylkin and Saito [11]). We choose the order 5 as a compromise between the requirement on continuity of the second derivative (which we will need later) and the demand to have the support as small as possible. The correlation function of Daubechies scaling function of order 5 and its Fourier transform $\Psi(\xi) = \int_{-\infty}^{+\infty} \psi(x) e^{-i\xi x} \, dx$ are shown in Fig. 2. Note that for symmetrical functions the imaginary part of the Fourier transform is always zero.

2.2. Interpolation on an Irregular Grid

The absolute value of the wavelet coefficient c_k^j appearing in the approximation (1) and computed in (3)

depends upon the local regularity of $u(x)$ in the neighborhood of location b_k^j. As mentioned in [1], numerical results indicate that for appropriately chosen N_l and N_r the method converges uniformly with increasing J. This indicates a decay of the magnitude of wavelet coefficients as the level of resolution increases. For the algorithm presented in [1] we show a typical collocation grid using a seven-level approximation. This grid, reproduced in Fig. 3b, is used regardless of the approximation function, assuming it can resolve all the scales present in the function. It seems that for a function which has singularities or sharp transitions, it is far from the optimal representation. In Fig. 3a we illustrate a function defined on the interval $[-1, 1]$ which has a sharp transition. For this function we present in Fig. 3c the grid of collocation points of the correlation function of the Daubechies scaling function of order 5 with coefficients whose absolute value is larger than a threshold $\varepsilon = 5 \times 10^{-3}$. We see a pyramid of collocation points that marks the location of the sharp transition. The width and height of the pyramid depend mostly on the magnitude of the gradient of $u(x)$, the size of the wavelet support, and the type of wavelet. In our case, out of the 275 collocation points (shown in Fig. 3b) only the 34 (shown in Fig. 3c) correspond to the wavelet coefficients which are above the threshold. This example indicates the tremendous saving if we design the algorithm to automatically take into account the structure of the approximated function.

The approximation (1) can be rewritten as a sum of two terms composed of wavelets whose amplitudes are above and below the threshold ε:

$$u^J(x) = u_\ge^J(x) + u_<^J(x), \tag{13}$$

where

$$u_\ge^J(x) = \sum_{j=0}^{J} \sum_{\substack{k \in Z^j \\ |c_k^j| \ge \varepsilon}} c_k^j \psi_k^j(x), \quad u_<^J(x) = \sum_{j=0}^{J} \sum_{\substack{k \in Z^j \\ |c_k^j| < \varepsilon}} c_k^j \psi_k^j(x). \tag{14}$$

Let us formulate and prove the following proposition.

PROPOSITION 1. *For any $\varepsilon > 0$ there exists a positive constant $\tilde{C}$ such that $\|u^J(x) - u_\ge^J(x)\|_{L^2(\Omega)} = \|u_<^J(x)\|_{L^2(\Omega)} \le \varepsilon \tilde{C}$.*

Proof.

$$\|u_<^J(x)\|_{L^2(\Omega)} = \left\| \sum_{j=0}^{J} \sum_{\substack{k \in Z^j \\ |c_k^j| < \varepsilon}} c_k^j \psi_k^j(x) \right\|_{L^2(\Omega)}$$

$$\le \sum_{j=0}^{J} \sum_{\substack{k \in Z^j \\ |c_k^j| < \varepsilon}} |c_k^j| \, \|\psi_k^j(x)\|_{L^2(\Omega)} \le \varepsilon N_W \|\psi(\xi)\|_{L^2(R)},$$
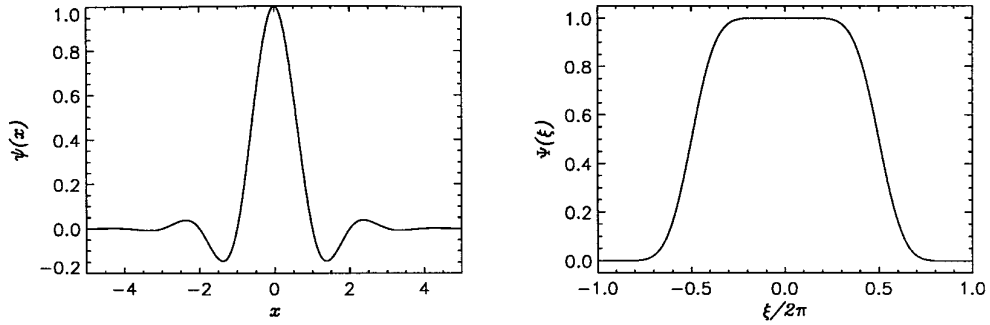
FIG. 2. The correlation function of the Daubechies scaling function of order 5 ($\psi(x)$) and its Fourier transform ($\Psi(\xi)$).

where N_W is the total number of wavelets. The last inequality follows since $|c_k^j| < \varepsilon$ and $\|\psi_k^j(x)\|_{L^2(\Omega)} \le \|\psi(\xi)\|_{L^2(R)}$. ∎

The estimate for the constant $\tilde{C}$ can be made much less conservative at the expense of complicating the proof. Consequently, Proposition 1 allows us to omit wavelets whose coefficients are below a certain threshold, and if we keep in approximation (1) only coefficients which are above the threshold, then we will still retain a good approximation. Due to the collocation nature of the algorithm we are interested in the L^∞ norm of the error and, since the magnitude of wavelet $\psi_k^j(x)$ is of the order $a_j^{-1/2}$, we only retain wavelets whose amplitude satisfy the criteria

$$|c_k^j| \ge a_j^{1/2}\varepsilon. \tag{15}$$

Note that by omitting a wavelet whose amplitude is below the threshold, the collocation point associated with this wavelet should be omitted as well. We call the grid of collocation points an irregular grid $\mathscr{G}_\ge$ if at least one collocation point at any level of resolution is omitted. Otherwise we will call it a regular grid $\mathscr{G}$. Examples of regular and irregular grids of wavelet collocation points are presented respectively in Figs. 3b and 3c. Note that the irregular grid becomes a regular one by setting the threshold parameter ε to zero.
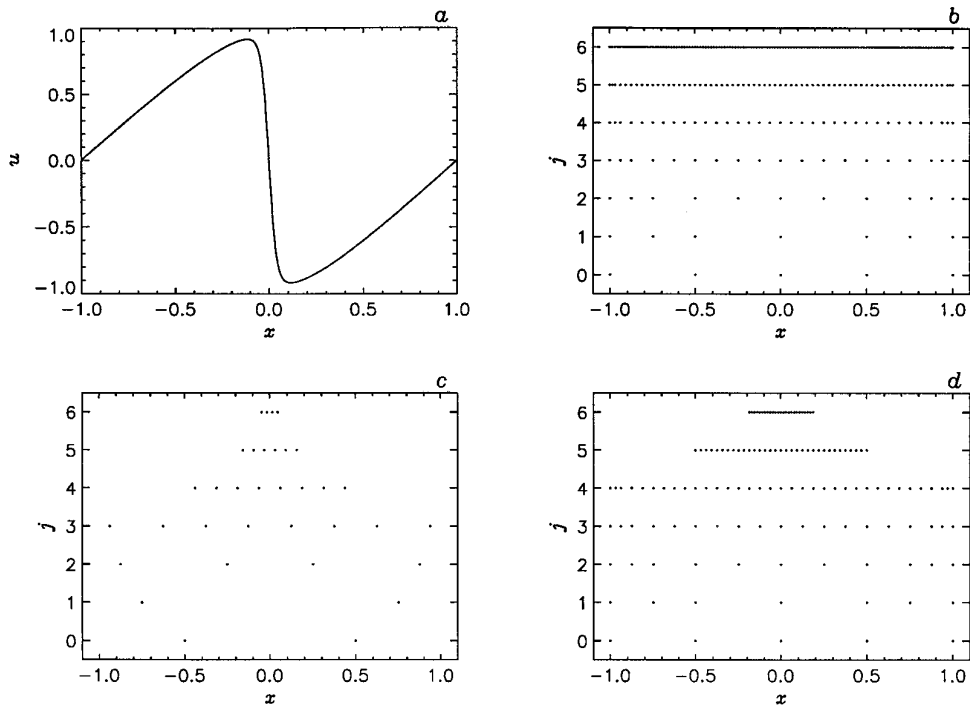

FIG. 3. (a) Function $u(x)$, (b) regular grid ($\varepsilon = 0$), (c) irregular grid ($\varepsilon = 5 \times 10^{-3}$, $M = 0$, $C = 0$), (d) irregular grid ($\varepsilon = 5 \times 10^{-3}$, $M = 1$, $C = 1$) of wavelet collocation points used in approximating the function.

If we look closely at Fig. 3c we see that the relation (2) between collocation points at different levels is violated. However, the algorithm on the irregular grid can be formally interpreted as the algorithm on a regular one where the coefficients which are below the threshold are set to zero. Let us define two subsets of integers $Z_{\geq}^j \subset Z^j$ and $Z^C \subset Z^J$ such that $x_i^j \in \mathcal{G}_{\geq}$ if and only if $i \in Z_{\geq}^j$ and $x_k^J \in \bigcup_{j=0}^J \{x_m^j : m \in Z_{\geq}^j\}$ if and only if $k \in Z^C$. In other words, $Z_{\geq}^j$ is the set of indices of wavelets (and collocation points) at the j level of resolution, and Z^C is the set of indices of the ultimate set of collocation points used in the interpolation. Subsequently, Eqs. (3), (4), (6), (10), and (11) can be rewritten as

$$c_k^j = \sum_{m \in Z^C} \mathbb{C}_{k,m}^{j,J} u_m^J, \quad 0 \leq j \leq J, k \in Z_{\geq}^j, \quad (16)$$

$$\mathbb{C}_{k,m}^{j,J} = \sum_{p \in Z_{\geq}^j} (A^{j,j})_{k,p}^{-1} \Delta_{p,m}^{j,J},$$

$$0 \leq j \leq J, k \in Z_{\geq}^j, m \in Z^C, \quad (17)$$

$$\Delta_{i,m}^{j,J} = \begin{cases} R_{i,m}^{j,J} - \sum_{l=0}^{j-1} \sum_{p \in Z^C} \sum_{k \in Z_{\geq}^l} R_{i,p}^{j,J} A_{p,k}^{J,l} \mathbb{C}_{k,m}^{l,J}, \\ \qquad\qquad 1 \leq j \leq J, i \in Z_{\geq}^j, m \in Z^C, \\ R_{i,m}^{0,J}, \qquad j = 0, i \in Z_{\geq}^0, m \in Z^C, \end{cases} \quad (18)$$

$$u^{J(m)}(x) = \sum_{i \in Z^C} D_i^{(m)}(x) u_i^J, \quad (19)$$

$$D_i^{(m)}(x) = \sum_{j=0}^J \sum_{k \in Z_{\geq}^j} \psi_k^{j(m)}(x) \mathbb{C}_{k,i}^{j,J}, \quad i \in Z^C. \quad (20)$$

Equations (16)–(20) can be formally obtained by substituting the sets of the subscripts $Z_{\geq}^j$ and Z^C, instead of Z^j and Z^J, respectively. Note that in the process of this formal substitution, $Z_{\geq}^J$ is substituted everywhere, where Z^j appeared for $j = J$, and Z^C, where Z^J appears explicitly. Also note that the size of the matrix $\mathbf{A}^{j,j}$ is determined by the number of elements in the set $Z_{\geq}^j$.

Since the main objective of this work is to use an irregular grid in an adaptive algorithm for solving partial differential equations, we will not elaborate any further on the influence of all the parameters associated with the algorithm on the interpolation characteristics. For this purpose we refer the reader to [1] for the case where $\varepsilon = 0$.

3. THE DYNAMICALLY ADAPTIVE ALGORITHM

The treatment of general boundary conditions on a finite domain is one of the difficulties for most wavelet algorithms. In [1] two different approaches of dealing with boundary conditions are suggested. The first is the derivative approach and the second is the integral approach. Since the objective of this paper is to present an adaptive algorithm, we will illustrate it using the derivative approach only, keeping in mind that the same adaptive procedure with slight modifications can be applied with the integral approach as well. We also note that in general the integral adaptive approach requires more degrees of freedom than the derivative one. This is due to the fact that extended wavelets, which are used in the integral approach, have larger support than regular wavelets once they are close to the boundary of the domain.

We will demonstrate the method through its application to the solution of a second-order partial differential equation of the type

$$\frac{\partial u}{\partial t} = F(t, x, u, u_x, u_{xx}) \quad \text{for } t > 0, u(x,0) = u_0(x), \quad (21)$$

where F is a linear or nonlinear operator. We illustrate the method by solving (21), together with the Dirichlet boundary conditions,

$$u(x_l, t) = u_l(t), \quad u(x_r, t) = u_r(t). \quad (22)$$

The time integration algorithm can be chosen depending on the applications. It can be either explicit or implicit. For some applications it can be mixed. For example, in many applications in fluid mechanics the Adams–Bashforth scheme is used for nonlinear terms and the Crank–Nicolson scheme is used for the linear terms. In our work we do not concentrate on the time integration scheme, since we want to focus on the adaptation in scale and space, retaining the freedom to choose the integration algorithm which is most appropriate for the particular application. In the present research we use a fifth-order Gear implicit integration algorithm implemented in the IMSL routine IVPAG [12].

We refer to the present method as *dynamically adaptive* in the sense that the irregular grid of collocation points is dynamically adapted in time and follows the local structures that appear in the solution. Let us describe the way we adapt the computational grid in time. The most straightforward approach for dynamical adaptation of the irregular grid is to retain only those collocation points for which the magnitude of associated wavelet coefficients satisfy criteria (15). Even though this approach works in interpolation problems, it is not applicable in the solution of partial differential equations for the following two reasons: the first reason is that, due to the finite support of wavelet and the recursive character of the algorithm, any change in a wavelet coefficient affects adjacent wavelets at the same and finer levels of resolution; the second reason is that, in order for the algorithm to be able to track sharp transitions

in the solution, we have to retain wavelets whose amplitude can possibly become significant during the next time interval. Both reasons suggest that we retain collocation points associated with wavelets that are adjacent in location and scale. Thus, at any instant of time the grid of wavelet coefficients should include wavelets belonging to an *adjacent zone*. We say that the wavelet ψ_k^s belongs to the adjacent zone of wavelet ψ_i^j (i.e., for which criteria (15) is satisfied), if the following relations are satisfied

$$|s - j| \le M, \quad |x_k^s - x_i^j| \le Ca_j, \tag{23}$$

where C defines the width of the adjacent zone in physical space and M determines the extent of which coarser and finer scales are included into the adjacent zone. In Fig. 3d the irregular wavelet collocation grid for the function shown in Fig. 3a is obtained with $C = 1$ and $M = 1$. Note that, as discussed earlier, the irregular wavelet collocation grid shown in Fig. 3c corresponds to the case with $C = 0$ and $M = 0$.

The values of C and M affect the total number of collocation points present in the irregular grid at any instant of time and the time interval during which the calculations can be carried out without modifying the computational grid and subsequently the matrix operators required in the computations. Note that in order to have an efficient algorithm we want to keep the number of collocation points as small as possible while at the same time we want to be able to resolve all sharp transitions present in the solution. Furthermore, for efficiency reasons we would like to minimize changes in the collocation grid. If $\tau_s(x_k^j)$ is the time scale of development coarser a_{j-1} or finer scale a_{j+1} in the neighborhood of x_k^j, and $\tau_c(x_k^j) = Ca_j/v(x_k^j)$, where $v(x_k^j)$ is local convection speed, then the time interval during which the computational grid can be kept unchanged is determined by $\tau = \min_{j,k}(\tau_s(x_k^j), \tau_c(x_k^j))$. For convenience we denote $\tau_1 = \min_{j,k}(\tau_s(x_k^j))$ and $\tau_2 = \min_{j,k}(\tau_c(x_k^j))$. In other words, in problems for which the convection time scale τ_2 is much larger than the time scale associated with development of sharp transitions τ_1, the value of C should be taken larger than in problems for which sharp transitions develop on a time scale much smaller than the one associated with convection. As far as the value of M is concerned, we found that the choice of $M = 1$ is the best compromise between requirements to minimize the number of collocation points and upgrade the computational grid as rare as possible.

Let us denote by $\mathscr{G}_{\ge}^t$ the irregular grid of wavelet collocation points that are retained to approximate the solution at time t. Following the classical collocation approach and evaluating (19), (20) at collocation points $\{x_i^J : i \in Z^C\}$ at the finest level of resolution we obtain

$$u_i^{J(m)}(t) = \sum_{k \in Z^C} D_{i,k}^{(m)} u_k^J(t), \tag{24}$$

$$D_{i,k}^{(m)} = \sum_{j=0}^{J} \sum_{p \in Z_{\ge}^j} \psi_p^{j(m)}(x_i^J) \mathbb{C}_{p,k}^{j,J}, \tag{25}$$

where $i \in Z^C$ and $\mathbb{C}_{p,k}^{j,J}$ is given by (17). From (12) it follows that

$$x_{-2^{L+J-1}-N_l}^J = x_l, \quad x_{2^{L+J-1}+N_r}^J = x_r, \tag{26}$$

and (21) reduces to a system of nonlinear ordinary differential equations,

$$\frac{d}{dt} u_i^J(t) = F(t, x_i^J, u_i^J(t), D_{i,k}^{(1)} u_k^J(t), D_{i,k}^{(2)} u_k^J(t)),$$
$$u_i^J(0) = u_0(x_i^J), \tag{27}$$

where $i \in Z^C$ and repeated indices imply summation over Z^C. The boundary conditions (22) become

$$u_{-2^{L+J-1}-N_l}^J(t) = u_l(t), \quad u_{2^{L+J-1}+N_r}^J(t) = u_r(t). \tag{28}$$

After solving (27) with boundary conditions (28), the solution on the interval is approximated by

$$u^J(x, t) = \sum_{i \in Z^C} I_i(x) u_i^J(t). \tag{29}$$

Note that for Neumann or mixed boundary conditions, (28) is replaced by an algebraic relation in terms of u_i^J, $i \in Z^C$. Thus one has to solve a differential–algebraic system of equations, which can be rewritten as a system of coupled ordinary differential equations by expressing the values of the function at the end points in terms of its values at the interior locations.

Let us summarize the numerical algorithm. Assuming that a time integration scheme is chosen, the present numerical algorithm involves three steps:

1. Assume we have computed the approximate solution $u_i^J(t)$ at positions on the irregular grid $\mathscr{G}_{\ge}^t$ (from initial conditions or from the previous time step). For a given threshold ε we adjust $\mathscr{G}_{\ge}^{t+\Delta t}$ based on the magnitude of wavelet coefficients at time t which are obtained using (16).

2. If $\mathscr{G}_{\ge}^t$ and $\mathscr{G}_{\ge}^{t+\Delta t}$ are the same go to step 3; otherwise:
   a. values of the solution $u_i^J(t)$ at collocation points of $\mathscr{G}_{\ge}^{t+\Delta t}$, which are not included in $\mathscr{G}_{\ge}^t$, are computed using (29), and
   b. recalculate operator $\mathbb{C}_{p,k}^{j,J}$ and the derivative matrix $D_{i,k}^{(m)}$ using (17) and (25), respectively.

3. Integrate (27) to obtain new values $u_i^J(t + \Delta t)$ at positions on the irregular grid $\mathscr{G}_{\ge}^{t+\Delta t}$, and go back to step 1.

The basic hypothesis behind this algorithm is that during a time interval Δt, the domain of wavelets with significant coefficients does not move in phase space beyond the border of the irregular grid. With such an algorithm the irregular grid of wavelet collocation points is dynamically adapted in time and follows the local structures that appear in the solution. The accuracy in the adaptive multilevel wavelet algorithm depends upon the threshold parameter ε. In addition, other parameters such as L, J, b_0, N_l, N_r, and the choice of wavelet affect the performance of the algorithm for fixed ε. If all parameters are appropriately chosen, so that all the scales present in the problem are resolved, then the accuracy of the method is determined solely by ε. The accuracy of the algorithm is increased with the decrease of ε until it reaches a limit determined by J. In this case in order to further increase the accuracy by decreasing ε, J should be increased first. In other words for each J there exists ε_J such that, in order for the approximation error to be determined by ε, the threshold parameter must satisfy the inequality $\varepsilon \geq \varepsilon_J$.

Note that the most computationally expensive part of the proposed algorithm is recalculating matrices $\mathbb{C}_{p,k}^{j,J}$ and $D_{i,k}^{(m)}$. If N^C is the total number of collocation points and M_W is the parameter which depends on the support (or effective support) of the wavelet (M_W effectively defines the bandwidth of the matrices $A_{i,k}^{j,j}$, $A_{i,k}^{J,j}$, $\psi_k^{j(m)}(x_i^J)$), then the upper bound of the total number of operations involved in calculating the matrix operators is given by $C_1 M_W N^C$ ($M_W + C_2 N^C$) and the storage requirement based on the matrix structures is $C_3 N^C (M_W + C_4 N^C)$, where the coefficients C_i ($i = 1, ..., 4$) are of order 1. In contrast with the nonadaptive algorithm [1], where these matrices are calculated only once, here whenever the irregular grid $\mathcal{G}_{\geq}^t$ changes these matrices have to be recalculated. However, because of the substantial decrease in the number of collocation points on each level of resolution in comparison with the nonadaptive approach, the resulting algorithm is considerably more efficient. In addition, the numerical procedure can be organized very efficiently by appropriately modifying the previously known matrices whenever additional wavelets or collocation points are added.

4. RESULTS AND DISCUSSION

In order to test the ability of the numerical algorithm to resolve rapid and localized variations in the solution, we consider three different problems. The first problem tests the ability to resolve a shock which is fixed in space but whose gradient changes in time. The second problem tests the ability to resolve a moving shock. The third problem illustrates the ability of the algorithm to be successfully applied to more complicated problems.

The rest of the section is organized as follows. In the first subsection we discuss the problem formulations and in the second we present numerical results. In both subsections, because of the fact that the first two problems have analytical solutions with which we can more rigorously check the algorithm, we split the discussion into two parts. In the first part we discuss the performance of the algorithm and its competitiveness with other numerical methods based on the results of the first two test problems. In the second part we illustrate the application of the present algorithm to the solution of third problem.

4.1. Problem Formulations

I. *Burgers Equation.*   For the first test problem we consider the Burgers equation

$$\frac{\partial u}{\partial t} + u \frac{\partial u}{\partial x} = \nu \frac{\partial^2 u}{\partial x^2}, \quad x \in (-1, 1), t > 0, \quad (30)$$

with initial and boundary conditions

$$u(x, 0) = -\sin(\pi x), \quad u(\pm 1, t) = 0 \quad (31)$$

whose analytical solution is known (see [13]). Also note that the boundary conditions at the two ends are of Dirichlet type and, since the wavelets that we utilize are symmetric, we use the same number of external wavelets on each side of the domain, i.e., $N_l = N_r = N$. In light of (27) and (28) the problem reduces to

$$\frac{d}{dt} u_i^J(t) = \sum_{k \in Z^C} [-u_i^J(t) D_{i,k}^{(1)} + \nu D_{i,k}^{(2)}] u_k^J(t),$$

$$u_i^J(0) = -\sin(\pi x_i^J), \quad (32)$$

$$u_{\pm(2^{L+J-1}+N)}^J(t) = 0,$$

where $i \in Z^C, i \neq \pm(2^{L+J-1} + N)$. The system (32) is solved with the fixed integration step $\Delta t = 5 \times 10^{-4}/\pi$.

II. *Modified Burgers. Equation.*   As a second test problem we consider the modified Burgers equation,

$$\frac{\partial u}{\partial t} + (v + u) \frac{\partial u}{\partial x} = \nu \frac{\partial^2 u}{\partial x^2}, \quad x \in (-\infty, +\infty), t > 0, \quad (33)$$

where v is a constant. The initial and boundary conditions are

$$u(x, 0) = -\tanh \left(\frac{x - x_0}{2\nu} \right), \quad u(\pm\infty, t) = \mp 1. \quad (34)$$

The analytical solution of this problem is a shock wave moving with the uniform velocity v given by

$$u(x, t) = -\tanh\left(\frac{x - x_0 - vt}{2\nu}\right). \qquad (35)$$

For numerical purposes, due to the exponential decay of the solution at infinity, the problem can be considered in a finite domain. Thus for $\nu = 10^{-2}$, $x_0 = -0.25$, $v = 1$, and $0 \le t \le 0.5$, it is legitimate to consider the problem in the domain $x \in [-1, 1]$ with Dirichlet boundary conditions. Analogous to the first test problem we take $N_l = N_r = N$. In light of (27) and (28) the problem reduces to

$$\frac{d}{dt} u_i^J(t) = \sum_{k \in Z^C} [-(v + u_i^J(t))D_{i,k}^{(1)} + \nu D_{i,k}^{(2)}] u_k^J(t),$$

$$u_i^J(0) = -\tanh\left(\frac{x_i^J - x_0}{2\nu}\right), \qquad (36)$$

$$u_{\pm(2^{L+J-1}+N)}^J(t) = \mp 1,$$

where $i \in Z^C$, $i \ne \pm(2^{L+J-1} + N)$. The system (36) is solved with the fixed integration step $\Delta t = 5 \times 10^{-4}$.

III. *Nonlinear Thermoacoustic Waves Problem.* As a third problem we consider a nonlinear thermoacoustic (TAC) wave problem. Below we just give the mathematical formulation of the problem. For details regarding the physical aspects of the problem we refer to [14]. Let us briefly describe the origin of the equations. Consider a compressible ideal gas between two rigid walls. The gas is initially quiescent at a uniform pressure and temperature. As a result of a temperature change at the left boundary, deviations from quiescent values will occur. We denote the nondimensional velocity, density, pressure, and temperature deviations by V, ρ, P, and T, respectively. The nondimensional continuity, momentum, energy, and state equations for the one-dimensional nonlinear TAC wave are given by

$$\frac{\partial \rho}{\partial t} + \frac{\partial V}{\partial x} + \frac{\partial(\rho V)}{\partial x} = 0, \qquad (37)$$

$$\frac{\partial V}{\partial t} + V\frac{\partial V}{\partial x} = -\frac{1}{\gamma(1 + \rho)}\frac{\partial P}{\partial x}$$

$$+ \frac{1}{\gamma(1 + \rho)}\frac{\partial}{\partial x}\left[\mu(T)\frac{\partial V}{\partial x}\right], \quad (38)$$

$$\frac{\partial T}{\partial t} + V\frac{\partial T}{\partial x} + (\gamma - 1)\frac{1 + P}{1 + \rho}\frac{\partial V}{\partial x}$$

$$= \frac{3}{4\text{Pr}(1 + \rho)}\frac{\partial}{\partial x}\left[k(T)\frac{\partial T}{\partial x}\right]$$

$$+ \frac{\gamma - 1}{1 + \rho}\mu(T)\left(\frac{\partial V}{\partial x}\right)^2, \qquad (39)$$

$$P = \rho + T + \rho T, \qquad (40)$$

where Pr is the Prandtl number, and γ is the ratio of specific heats, which is assumed to be temperature independent. Nondimensional viscosity and thermal conductivity are approximated by

$$\mu(T) = c_1\sqrt{1 + T} + c_2, \quad k(T) = c_3\sqrt{1 + T} + c_4. \quad (41)$$

The boundary conditions are

$$T(0, t) - T_w(t) = T(L, t) = V(0, t) = V(L, t) = 0 \quad (42)$$

and the initial conditions are

$$\rho(x, 0) = V(x, 0) = T(x, 0) = 0. \qquad (43)$$

The temperature at the left wall is taken to be $T_w(t) = AH(t)$, where $H(t)$ is the Heaviside function.

Analogous to the previous two problems we take $N_l = N_r = N$. In light of (27) and (28), the problem (37)–(43) reduces to

$$\frac{d}{dt}\rho_i^J = -\left(\frac{\partial V}{\partial x}\right)_i^J - \left(\frac{\partial(\rho V)}{\partial x}\right)_i^J, \qquad (44)$$

$$\frac{d}{dt}V_i^J = -V_i^J\left(\frac{\partial V}{\partial x}\right)_i^J - \frac{1}{\gamma(1 + \rho_i^J)}\left(\frac{\partial P}{\partial x}\right)_i^J$$

$$+ \frac{1}{\gamma(1 + \rho_i^J)}\left(\frac{\partial}{\partial x}\left[\mu(T)\frac{\partial V}{\partial x}\right]\right)_i^J, \qquad (45)$$

$$\frac{d}{dt}T_i^J = -V_i^J\left(\frac{\partial T}{\partial x}\right)_i^J - (\gamma - 1)\frac{1 + P_i^J}{1 + \rho_i^J}\left(\frac{\partial V}{\partial x}\right)_i^J$$

$$+ \frac{3}{4\text{Pr}(1 + \rho_i^J)}\left(\frac{\partial}{\partial x}\left[k(T)\frac{\partial T}{\partial x}\right]\right)_i^J$$

$$+ \frac{\gamma - 1}{1 + \rho_i^J}\mu(T_i^J)\left[\left(\frac{\partial V}{\partial x}\right)_i^J\right]^2, \qquad (46)$$

$$P_i^J = \rho_i^J + T_i^J + \rho_i^J T_i^J, \qquad (47)$$

$$T_{-(2^{L+J-1}+N)}^J(t) - T_w(t)$$

$$= T_{(2^{L+J-1}+N)}^J(t) = V_{\pm(2^{L+J-1}+N)}^J(t) = 0, \qquad (48)$$

$$\rho_i^J(0) = V_i^J(0) = T_i^J(0) = 0, \qquad (49)$$

where $i \in Z^C$ for Eqs. (44), (47), (49) and $i \in Z^C$, $i \ne \pm(2^{L+J-1} + N)$ for (45), (46), since the values for velocity and temperature at the boundaries are determined by (48). For clarity of presentation we denote

$$\left(\frac{\partial f}{\partial x}\right)_i^J = \sum_{k \in Z^C} D_{i,k}^{(1)} f_k^J. \tag{50}$$

Note that there are two different forms of the discretization of terms such as $(\partial/\partial x)(\mu(T)(\partial V/\partial x))$, the conservative form

$$\left(\frac{\partial}{\partial x}\left[\mu(T)\frac{\partial V}{\partial x}\right]\right)_i^J = \sum_{k \in Z^C} D_{i,k}^{(1)} \mu(T_k^J) \sum_{l \in Z^C} D_{k,l}^{(1)} V_l^J, \tag{51}$$

and the nonconservative form,

$$\left(\frac{\partial}{\partial x}\left[\mu(T)\frac{\partial V}{\partial x}\right]\right)_i^J = \mu(T_i^J) \sum_{k \in Z^C} D_{i,k}^{(2)} V_k^J$$
$$+ \frac{d\mu}{dT}(T_i^J) \sum_{k \in Z^C} D_{i,k}^{(1)} T_k^J \sum_{l \in Z^C} D_{i,l}^{(1)} V_l^J. \tag{52}$$

We find that both formulations lead to numerically indistinguishable results.

The problem is solved with $c_1 = 1.489$, $c_2 = -0.489$, $c_3 = 1.66$, $c_4 = -0.66$, $A = 1$, $\gamma = 1.4$, and $\text{Pr} = \frac{3}{4}$, which correspond to nitrogen gas at a reference temperature of 300 K. The system of Eqs. (44)–(49) is solved using an adaptive time integration step Δt such that $\Delta t \leq \tau$, where τ is the maximum time interval during which the computational grid can remain unchanged.

4.2. Numerical Results

Problems I and II. Basdevant *et al.* [13] presented a comparative study of spectral and finite difference methods for the solution of (30) and (31) with $\nu = 10^{-2}/\pi$. For such a small viscosity, the solution develops into a sawtooth wave at the origin for $t \gtrsim 1/\pi$. The gradient at the origin reaches its maximum value $|\partial u/\partial x|_{x=0}|_{\max} = 152.0051616$ at time $t_{\max} = 1.60369/\pi$. In the second test problem the region of large gradients is moving with the constant velocity v. The maximum value of the gradient is $|\partial u/\partial x|_{\max} = 1/(2\nu)$, which for $\nu = 10^{-2}$ becomes $|\partial u/\partial x|_{\max} = 50$. It appears from the study of Basdevant *et al.* [13] that the performance of a numerical method can be judged from its ability to resolve the large gradient regions that develop in the solutions, which are given in Fig. 4 for the first test problem and by (35) for the second one.

The dynamical adaptation of the solution and irregular grids $\mathscr{G}_{\geq}^l$ of wavelet collocation points is illustrated in Figs. 5 and 6 for first and second problems, respectively. In both cases we use the dynamically adaptive multilevel collocation method with the correlation function of the Daubechies scaling function of order 5 with $b_0 = 1.0$, $N = 1$ and threshold parameter $\varepsilon = 1 \times 10^{-3}$. The evolution
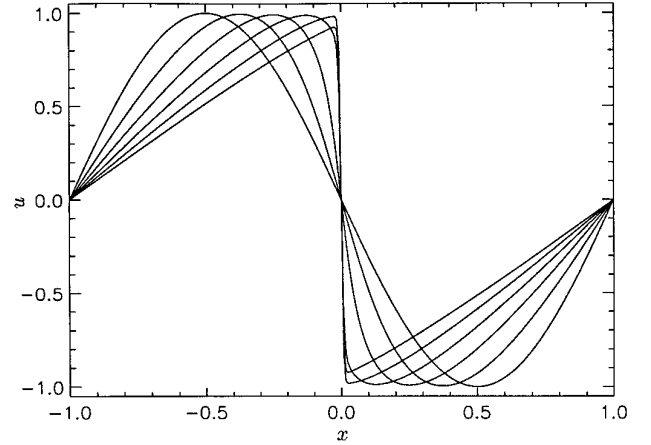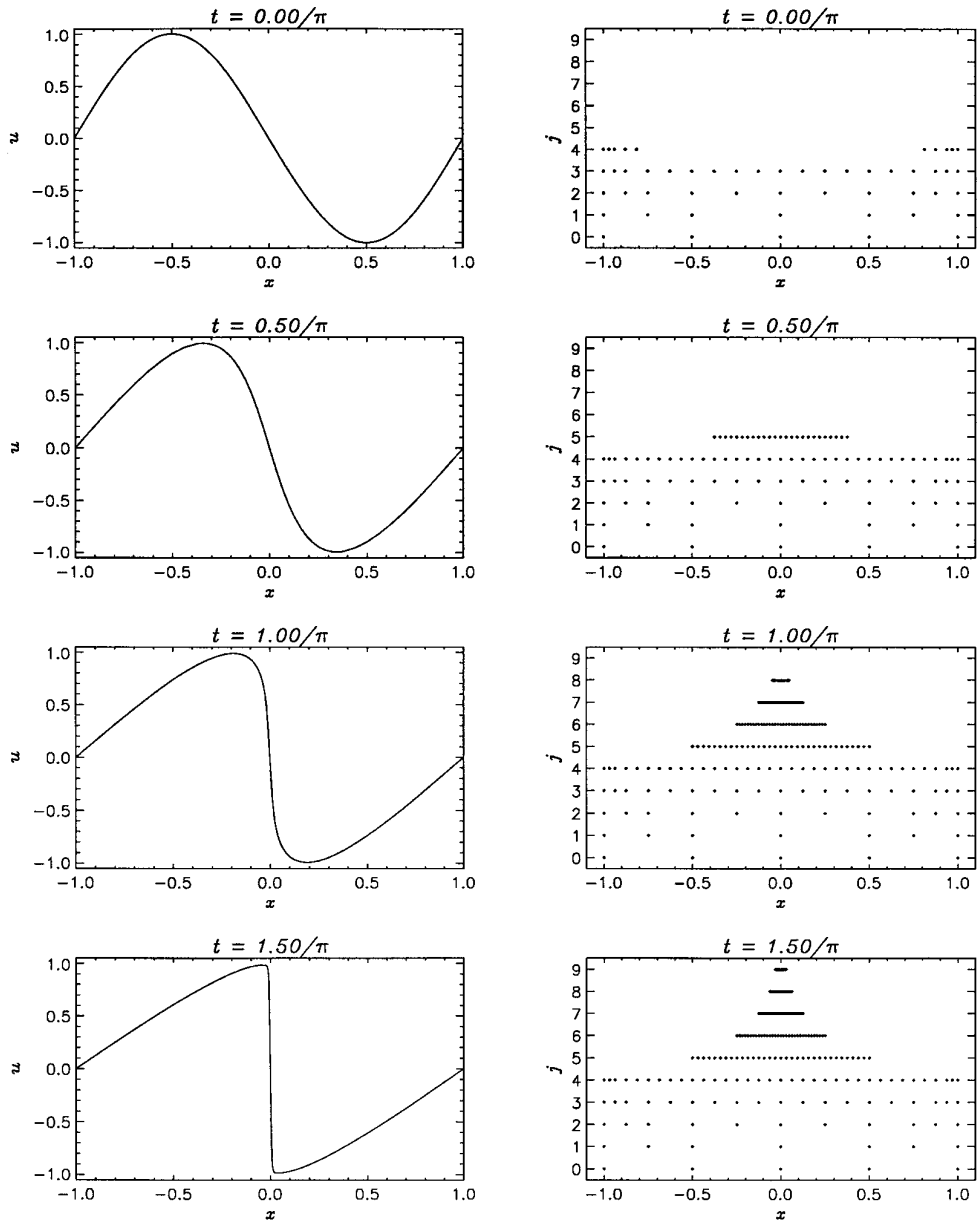

FIG. 4. Analytical solution of the Burgers equation at times $t = 2i/5\pi$, $i = O(1)5$.

of the solution of Burgers equation from the uniformly smooth distribution to the shock structure results in the growth of the wavelet coefficients corresponding to the smaller scales, which in turn results in the refinement of the grid. Figure 5 illustrates the progressive refinement of the irregular grid with the decrease of the shock thickness. In the second test problem we demonstrate that the algorithm dynamically adapts to the moving irregularities of the solution. Figure 6 shows that the region of collocation points associated with the small scales moves with the shock, thus permitting continuous proper resolution of the shock structure.

In Figs. 7a and b we show how the total number of collocation points N^C change with time for the first and second test problems. In Fig. 7a we note that N^C progressively increases with time until the gradient of the solution reaches its maximum. Then due to the viscous diffusion the value of the gradient decreases on a much slower time scale, which in turn results in a slow decrease of N^C. In Fig. 7b we see that the total number of collocation points oscillates around the average of $N^C = 101$. The reason for these oscillations is the sensitivity of the total number of collocation points on whether the shock is located at a collocation point or between collocation points.

The numerical results indicate that the biggest errors occur in the neighborhood of the shocks. Due to finite viscosity, the shock has a finite width. One would expect to resolve a shock properly if the scale associated with the finest level of resolution is smaller than the width of the shock. Since for our particular problem $b_0 a_J = 2^{1-L-J}$, then the shock can be resolved with sufficient accuracy with $L + J \geq 9$ in the first test problem and with $L + J \geq 7$ in the second one. For a more thorough discussion on this issue we refer to [1]. Note that even though the shock is resolved with $L = 1$, $J = 8$ and with $L = 1$, $J = 7$ in first
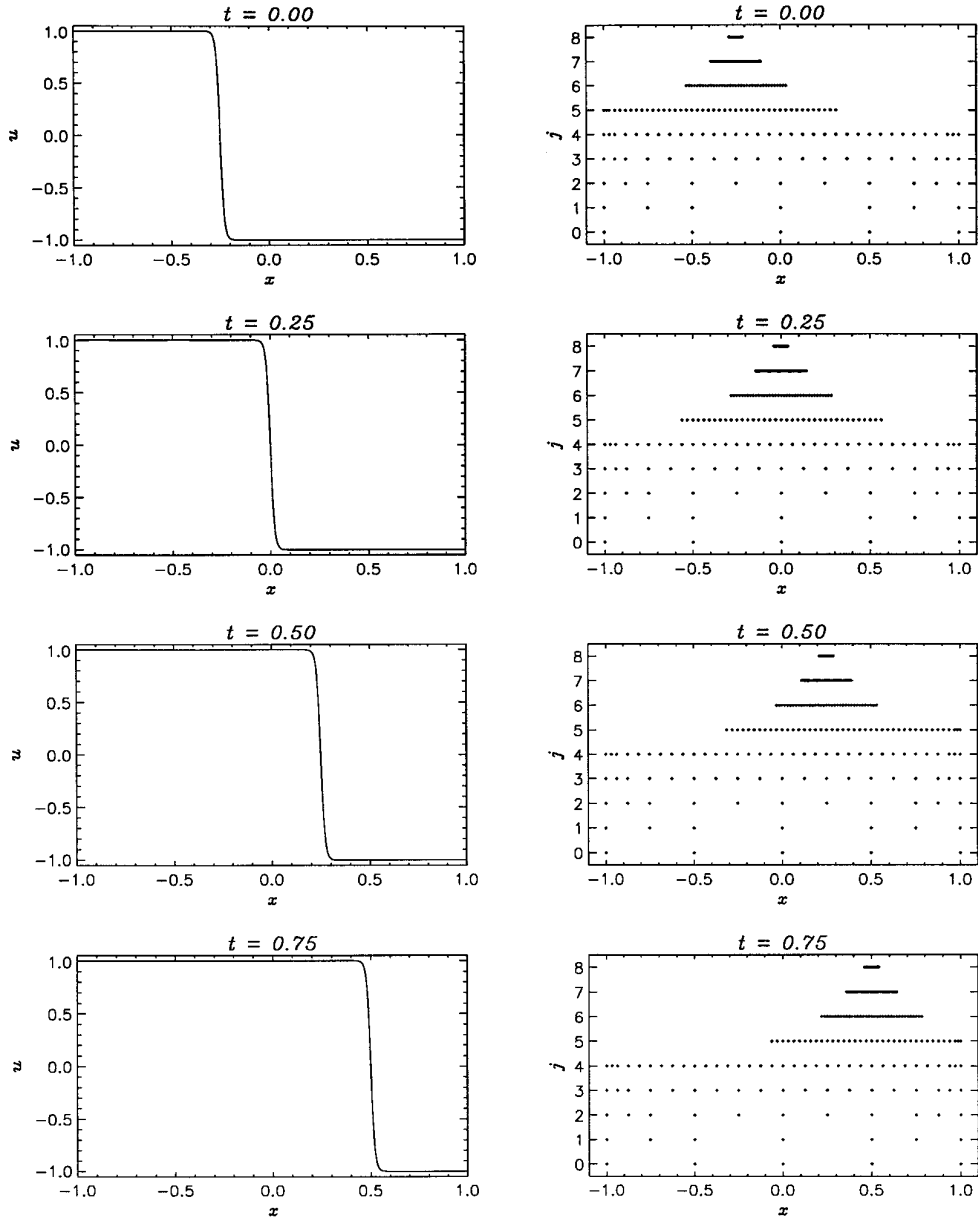
FIG. 5. Evolution of the solution (left column) and collocation points (right column) for the solution of the Burgers equation using the correlation function of the Daubechies scaling function of order 5.

and second test problems, respectively, the error in the neighborhood of the shock is determined by J in both cases ($\varepsilon < \varepsilon_J$ in these cases). Addition of an extra level decreases ε_J and changes the inequality to $\varepsilon > \varepsilon_J$, which in turn increases the accuracy of the solutions (see Tables I and II, cases 2 and 3).

The performance of the adaptive algorithm is strongly affected by the choice of wavelet. Although not given here, numerical results indicate that the adaptive algorithm using the correlation function of the Daubechies scaling function requires considerably fewer collocation points than using the Gaussian function or the Mexican hat wavelet. This phenomenon is associated with the localization properties of these bases. The Mexican hat wavelet has the worst localization, so that the adaptive algorithm utilizing it requires considerably more collocation points and, consequently, wavelets.

We emphasize that the multilevel approach is essential for an efficient adaptive algorithm. For fixed ε, with the decrease in number of levels of resolution the number of wavelets increases (see Tables I and II, cases 4–6). The algorithm becomes practically nonadaptive if only few lev-

FIG. 6. Evolution of the solution (left column) and collocation points (right column) for the solution of the modified Burgers equation using the correlation function of the Daubechies scaling of order 5.

els are utilized. This can be explained simply by the fact that more wavelets are required to approximate the large scales, which could be accomplished more effectively with fewer wavelets of larger scale.

Note that with an increase of the threshold parameter ε the number of collocation points decreases dramatically (see Tables I and II, cases 1, 2, 4). We point out that the algorithm becomes nonadaptive; i.e., it utilizes a regular grid, when ε is set to zero (Tables I and II, Case 1).

Summarizing the results presented in Tables I and II we see that the dynamically adaptive multilevel wavelet

collocation method ($\varepsilon > 0$) requires considerably fewer degrees of freedom than the nonadaptive method ($\varepsilon = 0$) without much loss in accuracy of the solution. This considerable reduction is achieved due to the local grid refinement which is done automatically based on the analysis of wavelet coefficients. With regard to the accuracy of the solution in comparison with those obtained with other numerical algorithms, we can say that for the same accuracy the adaptive multilevel wavelet collocation method requires substantially fewer degrees of freedom than spectral, finite difference, and nonadaptive wavelet Galerkin
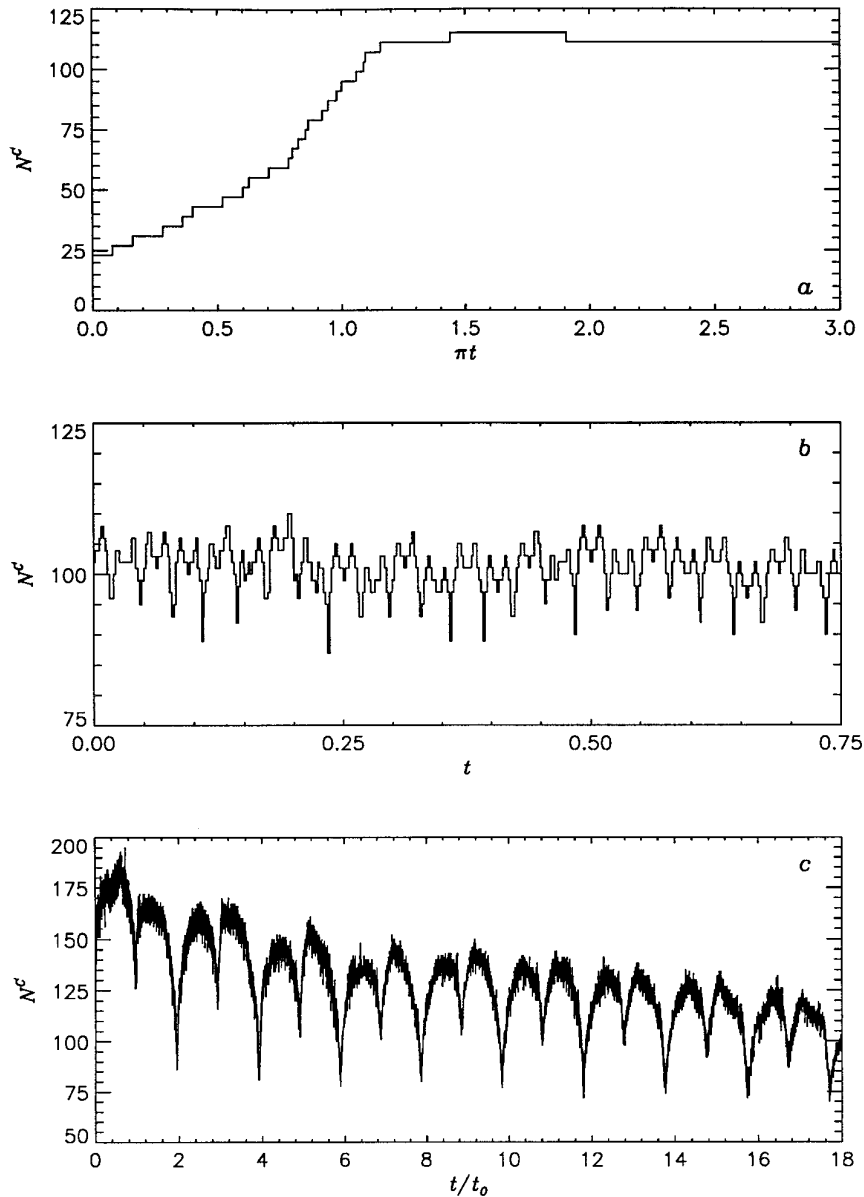
FIG. 7. Time evolution of the total number of collocation points N^C for (a) the first test problem with $M = 1$ and $C = 1$, (b) the second test problem with $M = 1$ and $C = 2$, (c) the third test problem with $M = 1$ and $C = 2$, using the correlation function of the Daubechies scaling function of order 5 and $\varepsilon = 1 \times 10^{-3}$.

schemes (see [1, 2]). In comparing the adapative wavelet Galerkin method of Liandrat and Tchamitchian [2] with the present algorithm, we observe that both require practically the same number of degrees of freedom to achieve comparable accuracy. However, the present algorithm has two clear advantages, in comparison with adaptive wavelet Galerkin algorithms. The first advantage is the simplicity in the treatment of general boundary conditions. The second is the handling of nonlinearities which requires only $O(N^C)$ operations, while the wavelet Galerkin algorithms require $O(n^2)$ operations [4], where n is the total number

of wavelets. In addition, treatment of nonlinear terms in partial differential equations leads to loss of accuracy due to the approximate calculation of scalar products using quadrature rules. For detailed discussion on the error associated with the use of quadrature formulas we refer to [8]. We also note that an adaptive wavelet Galerkin method cannot take advantage of the fast wavelet transform, unless the solution is interpolated to the finest uniform grid, as is originally done in [15]; but this procedure is even more computationally expensive. The only disadvantage of the present algorithm is the $O((N^C)^2)$ operations involved in

TABLE I

Numerical Results Obtained with the Present Algorithm for the Solution of Burgers Equation Using the Correlation Function of the Daubechies Scaling Function of Order 5 with $N = 1$ and $b_0 = 1.0$

	L	J	ε	Maximum number of collocation points	πt_{max}	Numerical $-(\partial u/\partial x)(0, t_{max})$	$\max_{x,t} |u - u^J|$
1	1	8	0	515	1.6030	149.28	1.72×10^{-3}
2	1	8	1×10^{-3}	99	1.6030	149.28	1.73×10^{-3}
3	1	9	1×10^{-3}	115	1.6035	151.90	1.04×10^{-4}
4	1	8	5×10^{-3}	95	1.6030	149.27	1.67×10^{-3}
5	6	3	5×10^{-3}	159	1.6035	149.32	1.91×10^{-3}
6	8	1	5×10^{-3}	515	1.6050	147.15	1.09×10^{-2}

calculations of matrix operators. But even with this disadvantage the present algorithm is very competitive with wavelet Galerkin algorithms for the solution of nonlinear problems.

Problem III. The thermoacoustic wave problem is fairly difficult to solve numerically because of the existence of two very different spatial scales present in the problem. The first scale is given by the size of the domain, while the second is associated with the nonlinear wave itself. Furthermore, for small time a small region of very large gradients exists close to the left wall.

Let us briefly discuss the evolution of the solution. The abrupt temperature change at the left wall generates a pressure wave, which propagates at the local speed of sound of the medium and gradually, over a long time scale, damps out because of thermal and viscous diffusion. Once the wave reaches a wall it reflects and propagates in the opposite direction. The process of reflection and diffusion continues until the wave dies out and a quiescent thermal conduction condition is achieved. For full discussion of this problem we refer to [16].

The dynamical adaptation of the solution and the irregular grid $\mathscr{G}_{\geq}^t$ of wavelet collocation points is illustrated in Fig. 8. The results are shown for the dynamically adaptive multilevel collocation method with the correlation function of the Daubechies scaling function of order 5 with $b_0 = 1.0$, $N = 1$ and threshold parameter $\varepsilon = 1 \times 10^{-3}$. From the figure we see that for small time, in order to resolve the region of sharp gradients, small scale wavelets are present in the approximation. With the time evolution of the solution the finest level of resolution gradually decreases. This is caused by the decreasing steepness of the wave due to heat and viscous diffusion. In addition, the fine levels of resolution are not present in regions far from the wave.

In comparison with the first two problems, which are described by single equations with one dependent variable, the thermoacoustic wave problem involves four unknowns, three partial differential equations (continuity, momentum, and energy), and one algebraic relation (equation of state). Thus the adaptation of the irregular grid $\mathscr{G}_{\geq}^t$ of wavelet collocation points is based on the analysis of coefficients associated with all the dependent variables. The irregular grid $\mathscr{G}_{\geq}^t$ is constructed as a union of irregular grids corresponding to each dependent variable. Note that the present algorithm can be easily extended to the case where each variable is treated on separate computational

TABLE II

Numerical Results Obtained with the Present Algorithm for the Solution of Modified Burgers Equation Using the Correlation Function of the Daubechies Scaling Function of Order 5 with $N = 1$ and $b_0 = 1.0$

|	L	J	ε	Maximum number of collocation points	Numerical $|\partial u/\partial x|_{max}$	$\max_{x,t} |u - u^J|$
1	1	7	0	259	49.86	4.31×10^{-4}
2	1	7	1×10^{-3}	94	49.86	4.95×10^{-4}
3	1	8	1×10^{-3}	110	50.00	$1\ 61 \times 10^{-4}$
4	1	7	5×10^{-3}	83	49.92	4.27×10^{-3}
5	5	3	5×10^{-3}	103	49.94	2.12×10^{-3}
6	7	1	5×10^{-3}	259	49.64	9.48×10^{-3}
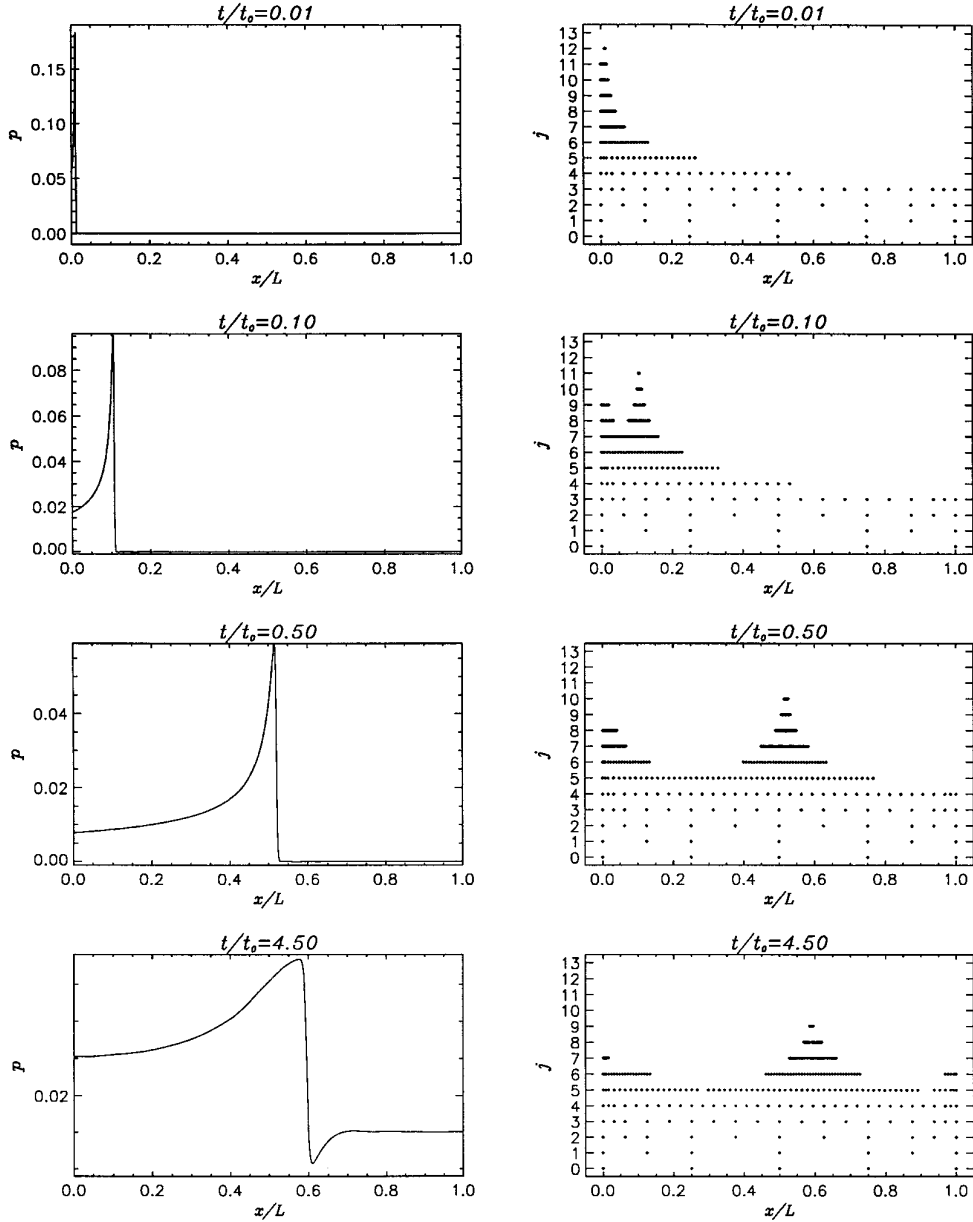
FIG. 8. Evolution of the pressure (left column) and collocation points (right column) for the one-dimensional nonlinear thermoacoustic wave problem with $t_0 = L = 13000$ and $A = 1$, using the correlation function of the Daubechies scaling function of order 5.

grids. The mapping from one grid to another can be achieved via wavelet interpolation. This may be very important for the problems where scales associated with the different variables are considerably different. In such a case the computational cost could be reduced substantially.

We also note that examination of the irregular grid gives information on the structure of the solution. For example, the irregular grid shown in Fig. 8 indicates the presence of a boundary layer at the left wall, which is not apparent in the pressure distribution. The presence of a boundary layer in density, temperature, and velocity profiles results

in the ultimate computational grid which reflects the presence of the boundary layer at the left wall. Were each variable solved on a separate grid, the computational grid for the pressure in the neighborhood of the left wall would not have collocation points corresponding to the fine levels of resolution.

In Fig. 7c we show the time evolution of the total number of collocation points N^C. The time interval for which the computational grid can be kept unchanged is much less than the time $t_0 = L$ associated with the wave traveling from one wall to another. Since the results in Fig. 7c are
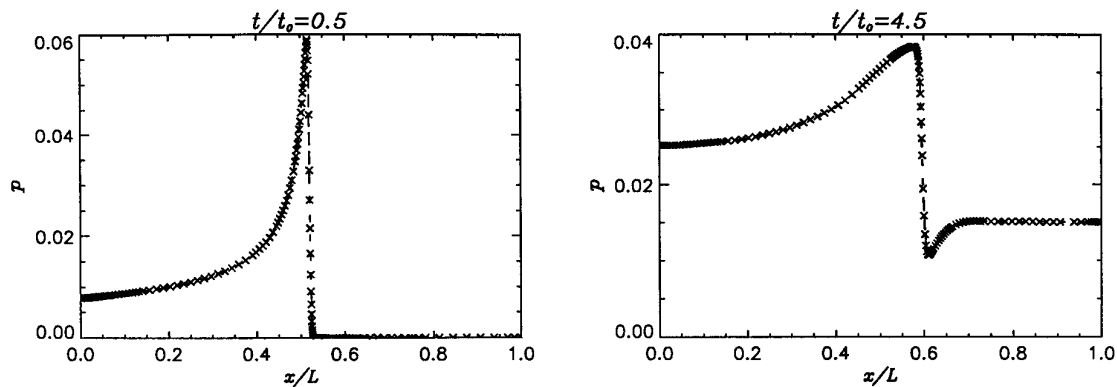
FIG. 9. Comparison of solutions at different times for the one-dimensional nonlinear thermoacoustic wave problem with $t_0 = L = 13000$ and $A = 1$ using the dynamically adaptive wavelet collocation method ($\times$) and a finite difference method (– – –) [16].

presented on a scale comparable with t_0, it is difficult to see the fast variations in N^C. Nevertheless we observe that the total number of collocation points gradually decreases, which is caused by the increase in the finest scale of the solution due to the thermal and viscous dissipations, and noticeable decreases in N^C are observed at times when the shock is in the neighborhood of a wall.

In Fig. 9 we present a comparison with the numerical result obtained by Huang and Bau [16] using a finite difference approximation on a uniform grid. In order to obtain the results shown in Fig. 9, they use 6000 grid points, while in our algorithm the number of collocation points did not exceed 195 at any time. In addition, small oscillations were observed in their solution at small times due to the unresolved scales associated with the initial large gradients.

5. CONCLUSIONS

A dynamically adaptive wavelet collocation method based on a wavelet interpolation technique is developed for the solution of partial differential equations in a finite domain. The method is tested on the one-dimensional Burgers equation, the modified Burgers equation with small viscosities, and a one-dimensional nonlinear thermoacoustic wave problem. The results indicate that the computational grid and associated wavelets can very efficiently adapt to the local irregularities of the solution in order to resolve regions of large gradients. The multilevel approach is essential for the present algorithm. The method can handle general boundary conditions. The present algorithm is not only very competitive with adaptive wavelet Galerkin algorithms, in addition it has distinctive advantages in the treatment of general boundary condition and nonlinearities.

Future areas of further development include the applica-

tion to two- and three-dimensional domains. This work is currently underway.

REFERENCES

1. O. V. Vasilyev, S. Paolucci, and M. Sen, *J. Comput. Phys.* **120,** 33 (1995).
2. J. Liandrat and P. Tchamitchian, NASA Contractor Report 187480, ICASE Report 90-83, NASA Langley Research Center, Hampton, VA 23665-5225, 1990 (unpublished).
3. E. Bacry, S. Mallat, and G. Papanicolau, *Math. Model. Numer. Anal.* **26,** 793 (1992).
4. Y. Maday and J. C. Ravel, *C. R. Acad. Sci. Paris* **315,** 85 (1992).
5. S. Bertoluzza, Y. Maday, and J. Ravel, *Comput. Methods Appl. Mech. Eng.* **116,** 293 (1994).
6. G. Beylkin, R. Coifman, and V. Rokhlin, Tech. Rep. YALEU/DCS/RR-696, Yale University, August 1989 (unpublished).
7. G. Beylkin, *SIAM J. Numer. Anal.* **29**(6), 1716 (1992).
8. W. Sweldens and R. Piessens, *SIAM J. Numer. Anal.* **31,** 1240 (1994).
9. Y. Meyer, *Ondelettes et opérateurs* (Hermann, Paris, 1990).
10. L. Andersson, N. Hall, B. Jawerth, and G. Peters, "Wavelets on a Closed Subsets of the Real Line," in *Recent Advances in Wavelet Analysis* (Academic Press, San Diego, 1993).
11. G. Beylkin and N. Saito "Wavelets, Their Autocorrelation Functions, and Multidimensional Representation of Signals," *in* Proceedings of SPIE—The International Society of Optical Engineering, Vol. LB26, Int. Soc. for Optical Engineering (Bellingham, 1993).
12. *IMSL Mathematical Library,* Version 1.1, 1989.
13. C. Basdevant, M. Deville, P. Haldenwang, J. M. Lacroix, J. Ouazzani, R. Peyret, P. Orlandi, and A. T. Patera, *Comput. & Fluids* **14,** 23 (1986).
14. Y. Huang and H. H. Bau, *Int. J. Heat Mass Transfer* **38,** 1329 (1995).
15. Y. Maday and J. C. Ravel, *C. R. Acad. Sci. Paris* **312,** 405 (1991).
16. Y. Huang and H. H. Bau, *Int. J. Heat Mass Transfer,* to appear.